Analysis of Dead-Time Harmonics in Single-Phase Transformerless Full-Bridge PV Inverters

Yongheng Yang*, *Senior Member, IEEE*, Keliang Zhou†, *Senior Member, IEEE*, and Frede Blaabjerg*, *Fellow, IEEE*

*Department of Energy Technology, Aalborg University, Aalborg 9220, Denmark
†School of Engineering, University of Glasgow, Glasgow G12 8QQ, United Kingdom
yoy@et.aau.dk; keliang.zhou@glasgow.ac.uk; fbl@et.aau.dk

***Abstract*—A short period, called dead time, is usually implemented (e.g., through adding extra hardware in gate drivers or modifying pulse-width modulation schemes) for voltage source inverters to prevent shoot-through incidents. Clearly, larger dead time provides more safety, but may also degrade the injected currents from inverters. It thus requires sophisticated compensation schemes to meet certain stringent standards. For single-phase transformerless full-bridge PV inverters, different modulation schemes can be employed to suppress leakage currents, which in return may affect the distribution of the dead time harmonics. Thus, this drives the analysis of dead time harmonics in single-phase transformerless full-bridge inverters considering two modulation strategies: bipolar and unipolar modulation schemes. Effects of modulation on the dead time harmonics are observed in simulations and experimental tests. Furthermore, a periodic controller is adopted to mitigate the harmonics, which is independent of the modulation schemes.**

***Index Terms*—Single-phase inverter, dead-time, bipolar modulation, unipolar modulation, harmonics, repetitive controller**

I. Introduction

Power electronics are the key to today's energy conversion [1]. Harmonics appear in power electronic-based power systems, and thus challenging the stability (i.e., system resonance may be triggered) [2]–[4]. There are two major reasons behind this: 1) the interaction of power converters with high nonlinearity and 2) the intermittent nature of generation (especially, for renewable energies). To tackle the harmonic issue in power electronic converters, the control should be advanced [5], [6], which enables a low Total Harmonic Distortion (THD) level. At the same time, many standards have been published to guide the connection of an increasing number of power electronic converters to the grid [7], [8]. Alternatively, through topological innovations, e.g., using high-order passive filters and multilevel converter technologies, harmonic emissions can be attenuated to some extent. Nonetheless, further attempts to mitigate harmonics are expected in future power electronic-dominated systems.

In practical applications, two-level voltage source converters are still the favorite for PV systems [1]. Furthermore, other issues like leakage currents should be considered. For instance, a short period, called dead time, has to be implemented in the Pulse Width Modulation (PWM) drivers or modulation strategies during each switching interval [9]–[13]. This is to avoid any shoot-through incident in the converter, and clearly, larger dead time is safer. Doing so, however, may lead to emission of more harmonics from the PWM converters [14], [15]. Specifically, the dead time may contribute to a decrease or increase of the fundamental component of the converter output [16]–[18]. The injected currents will then be further distorted [4], and additional losses may be observed. This dead time effect will be worse with a high switching frequency. In addition, for single-phase transformerless PV inverters, the PWM schemes should be designed to mitigate or prevent leakage currents. However, this may affect the distribution of dead time harmonics [19], [20].

The dead time harmonics have to be compensated in those applications. Prior-art methods are based on an average value theory [11], [16], [21], where the average voltage change is added to or subtracted by the inverter voltage reference. However, those methods rely on the detection of current polarity, and thus noise at zero-crossing of the current will degrade the compensation performance. Other solutions have also been reported in the literature [9]–[13], [16], [22]. For example, a compensation method using the controller integrator output and an adaptive dead time compensator were introduced in [16] and [22], respectively. Besides, since the dead time mainly introduces low order harmonics, it is possible to mitigate these harmonics using multiple resonant controllers and repetitive controllers [5], [15]–[17], [23]. Nonetheless, the dead time harmonic generation mechanisms are not clear when considering modulation strategies.

Therefore, this paper analyzes the harmonic distribution due to the dead time in single-phase transformerless full-bridge PV inverters. In § III, two modulation schemes - the bipolar and unipolar PWM schemes, are investigated considering 1) the leakage currents and 2) the dead time harmonics. The exploration reveals that the modulation schemes affect the harmonic characteristics of the injected currents. Simulations and experiments shown in § IV have validated the analysis. In addition, a repetitive controller based dead time compensation has been experimentally demonstrated on a single-phase PV inverter. Finally, § V concludes this paper.

II. Modulation Schemes

A grid-connected single-phase single-stage transformerless PV inverter system is shown in Fig. 1, where an LCL filter

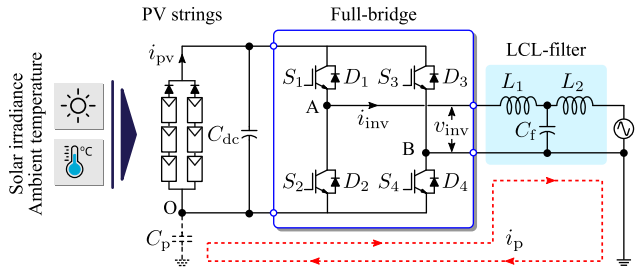

Fig. 1. A single-phase grid-connected transformerless PV inverter with an LCL filter, where C_p is the parasitic capacitance, i_p is the leakage current, and C_{dc} is the dc-link capacitance.

is adopted to remove switching-frequency harmonics. The dashed line with arrows indicates possible leakage current paths. One objective to design the modulation schemes is to minimize the leakage current i_p as

$$i_p = C_p \frac{dv_{cm}}{dt} = \frac{1}{2} C_p \frac{d(v_{AO} + v_{BO})}{dt} \tag{1}$$

where v_{cm} is the common-mode voltage, C_p is the parasitic capacitor, and v_{AO}, v_{BO} are the phase-leg output voltages. Clearly, the phase-leg output voltages are related to the modulation schemes.

In order to minimize the leakage currents, the modulation schemes should achieve a constant common-mode voltage (i.e., $v_{cm} = const.$) according to (1). For the single-phase full-bridge inverter, there are mainly two modulation schemes – bipolar modulation and unipolar modulation [24], as shown in Figs. 2 and 3. As observed, in the case of the bipolar modulation, the four power devices of the full-bridge inverter are switched in a diagonal way, i.e., S_1 synchronous with S_4 and S_2 with S_3; while two modulation signals with a phase shift of 180° are adopted to modulate each phase leg in the unipolar modulation. Thus, the inverter output voltage $v_{inv} = v_{AO} - v_{BO}$ will be different (i.e., two voltage states for the bipolar modulation and three voltage states for the unipolar modulation, as shown in Figs. 2 and 3, respectively).

Nevertheless, the performance of a single-phase full-bridge inverter is dependent on the two modulation schemes, as demonstrated in Fig. 4. It is observed in Fig. 4 that the bipolar modulation results in a constant common mode voltage v_{cm}. According to (1), the leakage current will be zero – the bipolar modulation is better in terms of low leakage currents compared with the unipolar modulation scheme. However, as two modulation signals are adopted, the phase shift will cancel the switching-frequency harmonics if the unipolar modulation scheme is adopted. This means that the unipolar modulation has an effect of double the switching frequency, leading to low requirements on the output filters. This effect will be demonstrated in § IV by simulations.

III. Dead-Time Harmonics

In the last section, it has been shown that the modulation schemes will alter the harmonic characteristics of the single-phase inverter output voltage (i.e., v_{inv}). When the dead time

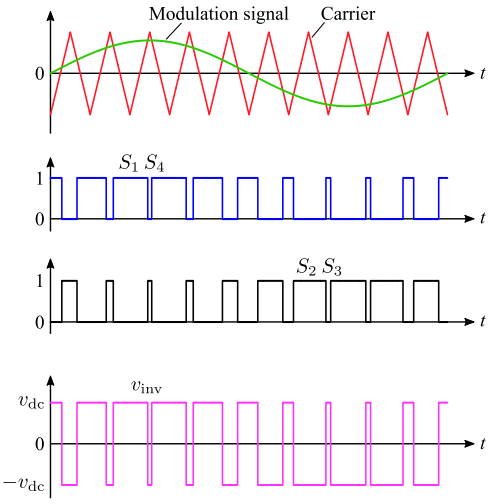

Fig. 2. Bipolar pulse width-modulation (PWM) strategy for the single-phase full-bridge inverter.

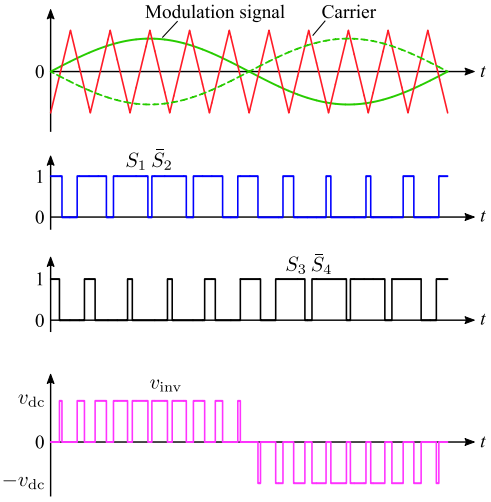

Fig. 3. Unipolar pulse width-modulation (PWM) strategy for the single-phase full-bridge inverter.

is inserted in each switching interval, the output voltage will be further affected. In this section, how the dead time affects the voltage is first presented. Then, a strategy to mitigate the dead time harmonics is given, in which a repetitive (periodic) controller is adopted.

A. Dead Time Effect with Different Modulations

For simplicity, the impact of dead time Δt on the inverter output voltage (i.e, $v_{inv} = v_{AO} - v_{BO}$) can be explained using one of the phase legs in Fig. 1. During one switching period, the modulation signal is assumed as constant, as it is shown in Fig. 5. In the dead time periods, the turn-on pulses are delayed, and thus the inverter output phase voltage v_{AO} is affected. This influence is related to the polarity of the inverter output current i_{inv}, as indicated in Fig. 5. More specifically, v_{AO} is increased (i.e., there is a voltage gain), if the phase output current i_{inv} is negative; otherwise, the inverter output phase voltage v_{AO} is

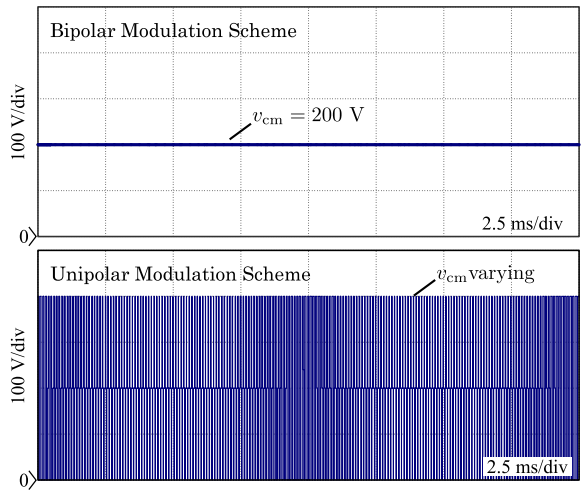

Fig. 4. Common mode voltage of the single-phase PV inverter shown in Fig. 1 with the two modulation schemes, where the voltage across the capacitor C_{dc} is fixed at 400 V.

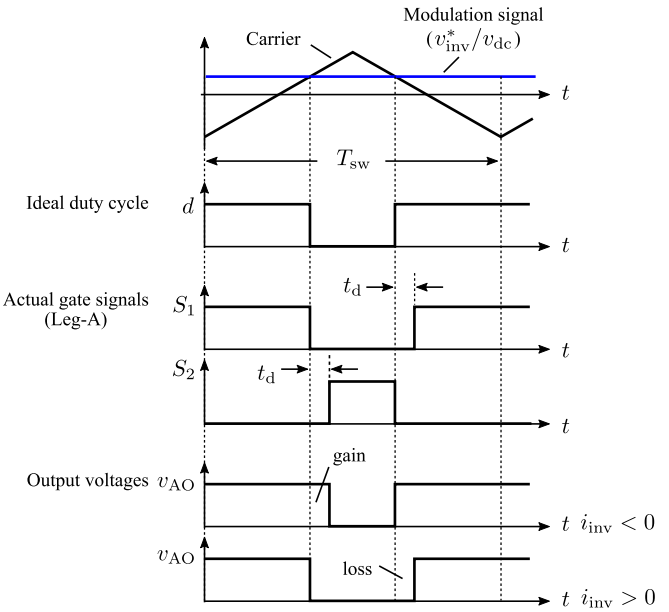

Fig. 5. Distortions of the leg-A output voltage of the full-bridge inverter shown in Fig. 1 due to the dead time, where v_{dc} is the dc-link voltage across the capacitor C_{dc}, v^*_{inv} is the inverter voltage reference from the current controller, t_d is the dead time, T_{sw} is the switching period, and i_{inv} is the inverter output current.

reduced (i.e., there is a voltage loss). In one switching period T_{sw}, the voltage difference Δv of the leg-A output can simply be averaged as

$$\Delta v \approx -sgn\left(i_{inv}\right) \cdot \frac{t_d}{T_{sw}} \cdot v_{dc} \tag{2}$$

with

$$sgn\left(i_{inv}\right) = \begin{cases} 1, & i_{inv} > 0 \\ -1, & i_{inv} < 0 \end{cases}$$

where T_{sw} is the switching period and v_{dc} is the instantaneous voltage across the dc-link capacitor C_{dc}. It is implied in (2) that the inverter output voltage will be distorted by the dead time. The larger the dead time t_d is, more severe the distortion is (i.e., the larger the voltage difference $|\delta v|$ is). Also a high switching frequency (i.e., a small switching period T_{sw}) leads to large distortions.

Similarly, the voltage distortions in the inverter leg-B can be obtained. For the single-phase full-bridge inverter shown in Fig. 1, with the bipolar modulation scheme, the voltage distortions of the leg-B will be identical to (2) but the current polarity is opposite. Then, it is easy to obtain the voltage distortion in the inverter output voltage v_{inv}. However, for the unipolar modulation scheme, the voltage difference in the output of leg-B can be obtained following the above, but the entire voltage distortion in the inverter output may be different. Thus, it is necessary to model the harmonics under different modulation schemes. Nevertheless, the distortions in the inverter output voltage will be propagated to the grid current [4] according to

$$i_g = \frac{1}{L}\int \left(v^1_{inv} - v_g\right) dt + \frac{1}{L}\int v^h_{inv} dt \tag{3}$$

in which $L = L_1 + L_2$ is the total inductance, v_g is the grid voltage and it is assumed as harmonic-free, i_g is the injected grid current, v^1_{inv} is the fundamental inverter output voltage, and v^h_{inv} is the dead time harmonics of the inverter output voltage. Thus, the grid current will contain harmonics as

$$i^h_g = \frac{1}{L}\int v^h_{inv} dt \tag{4}$$

with h being the harmonic order. Since the modulation schemes result in different output voltage harmonics v^h_{inv}, the injected grid current harmonics will be affected.

B. Mitigation of Dead-Time Harmonics

The harmonics induced by the dead time can still be expanded into Fourier series [15], [16]. Accordingly, it is possible to compensate the dead time harmonics by including a harmonic compensator in the current controller. Regarding the harmonic compensator, a multiple-parallel resonant controller or a repetitive controller can be adopted. The resonant controller enables selectively canceling out the harmonic components (thus, a model of the dead time harmonics is needed to specifically compensate the harmonics). In contrast, the repetitive controller can theoretically mitigate all harmonics below the Nyquist frequency. In both cases, the harmonic compensators should be added in parallel with the fundamental current controller. Fig. 6 shows the entire current control loop of the single-phase full-bridge inverter system with harmonic compensators.

Accordingly, the transfer functions of the fundamental-frequency controller and the harmonic compensators can be obtained as

$$G_{fund}(s) = k_p + \frac{k_i s}{s^2 + \omega_0^2} \tag{5}$$

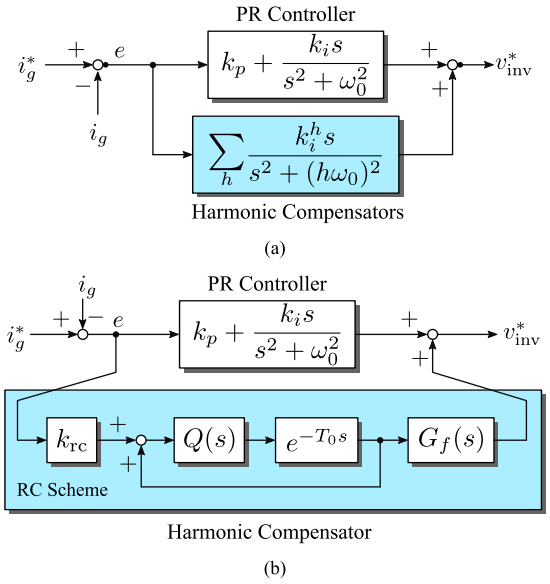

Fig. 6. Current control loop of the single-phase inverter with harmonic compensation to mitigate the dead time harmonics using: (a) multiple resonant controllers and (b) a repetitive controller.

being the fundamental-frequency current controller (i.e., a proportional resonant controller),

$$G_{\text{rsc}}(s) = \sum_h \frac{k_i^h s}{s^2 + \omega_h^2} \tag{6}$$

with $\omega_h = h\omega_0$, and

$$G_{\text{rc}}(s) = k_{\text{rc}} \frac{e^{-2\pi s/\omega_0} Q(s) G_f(s)}{1 - e^{-2\pi s/\omega_0 s} Q(s)} \tag{7}$$

being the harmonic compensators, where ω_0 is the fundamental frequency, k_p and k_i are the control gains for the fundamental-frequency current controller, k_i^h is the control gain for the hth-order resonant compensator, and k_{rc} is the control gain for the repetitive controller. In (7), a low pass filter $Q(s)$ and a phase-lead compensator $G_f(s)$ are adopted to enhance the control system stability. Additionally, as the expanded repetitive controller contains all the resonant controllers below the Nyquist frequency [5], it is efficient to use the repetitive controller to compensate the dead time harmonics. In that case, only one control gain (i.e., k_{rc}) should be tuned, but the controller can compensate a wide range of harmonics. Also the information of the dominant harmonics induced by dead time is not required. Hence, in this paper, the repetitive controller is employed.

IV. Results

Referring to Fig. 1, simulations and experiments have been performed on a 2-kW single-phase inverter to verify the impact of dead time. In the case study, a dc source has been adopted. The switching frequency is f_{sw} = 10 kHz. A proportional resonant (PR) controller is adopted as the fundamental-frequency current controller. The other parameters are listed in Table I. Fig. 7 shows the simulation results of the system without

TABLE I
System Parameters of the Single-Phase Full-Bridge Transformerless PV Inverter (see Fig. 1).

Parameter	Symbol	Value
Rated power	P_{n}	2 kW
DC-link voltage	V_{dc}	400 V
Grid voltage in RMS	V_{g}	230 V
Grid frequency	ω_0	$2\pi\times50$ rad/s
DC-link capacitor	C_{dc}	1100 μF
	L_1	3.6 mH
LCL filter	C_{f}	2.35 μF
	L_2	4 mH
Sampling frequency	f_{s}	10 kHz

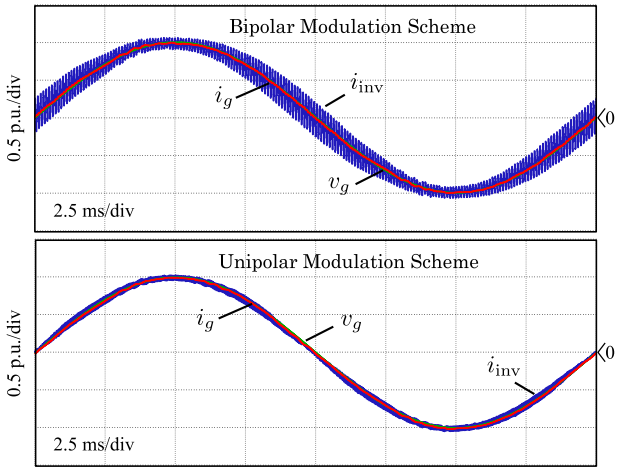

Fig. 7. Simulation results of the single-phase grid-connected transformerless inverter without dead time, where only the PR fundamental-frequency current controller is adopted.

dead time, which demonstrates the effectiveness of the PR controller. Moreover, it is seen in Fig. 7 that the output voltage ripples in the case of the unipolar modulation are smaller. This is because of the double switching frequency effect, as mentioned in § II. However, when the dead time of 5.25 μs is implemented, distortions in the inverter output voltage are observed, and thus in the injected grid current according to the above basic discussion. Fig. 8 verifies the impact of the dead time, where it can be seen that with different modulation schemes, the distortions are not the same. Notably, here, the large dead time is just to show the impact. In practice, the dead time duration is shorter. Nevertheless, it confirms that the modulation scheme will affect the distribution of dead time harmonics. To maintain the current injected by the PV inverter, harmonic compensation schemes should be adopted.

Experimental tests are then carried out, and the results are shown in Fig. 9, where the bipolar modulation scheme is adopted. It can be observed in Fig. 9 that the experimental results are in a close agreement with the simulations. When only the fundamental-frequency PR controller is adopted, the dead time harmonics will appear in the grid current, as seen in Fig. 9(a). In order to improve the current quality, a repetitive-

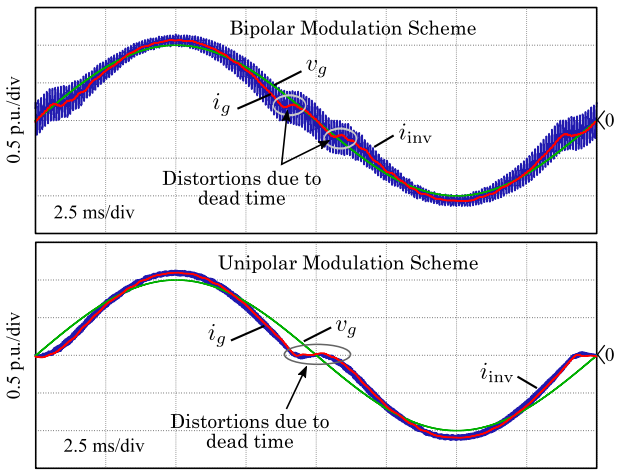

Fig. 8. Simulation results of the single-phase grid-connected transformerless inverter with the dead time being 5.25 μs, where only the PR fundamental-frequency current controller is adopted.

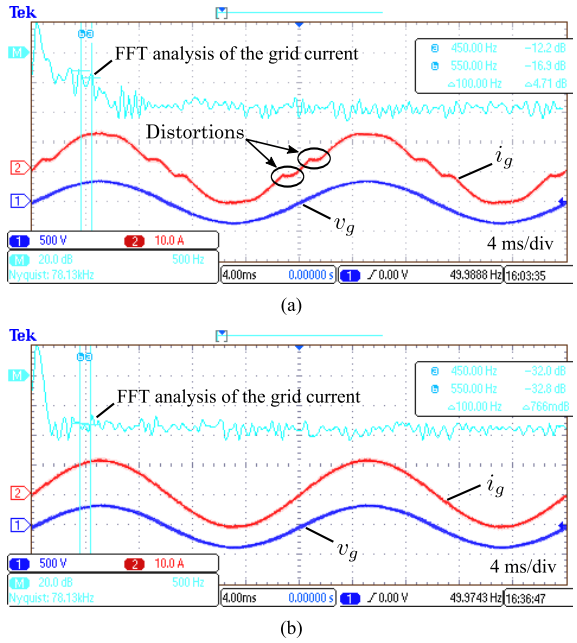

Fig. 9. Experimental results of the single-phase grid-connected transformerless inverter with the dead time being 5.25 μs (grid voltage - v_g [500 V/div], grid current - i_g [10 A/div], FFT - Fast Fourier Transform, FFT magnitude [20 dB/div], FFT frequency [500 Hz/div]): (a) without and (b) with the repetitive harmonic compensator. The bipolar modulation scheme is adopted considering the leakage currents.

based harmonic compensator is plugged into the current controller (i.e., in parallel with the PR controller) according to the discussions in § III and Fig. 6(b). As it is shown in Fig. 9(b), the dead time harmonics are effectively mitigated, when the repetitive controller is adopted. In the case of the unipolar modulation scheme, the harmonic distribution will be different. Thus, harmonic compensators should be designed according to the distribution. Nevertheless, the above cases have verified the analysis and discussions - the dead time harmonics are affected by the modulation strategies. It should be pointed out that the repetitive controller is also effective for the unipolar-modulated inverters, as it can a wide range of harmonics, being independent of the modulation schemes. However, the repetitive controller suffers from slow dynamics, and recent advancements of the repetitive controller are directed to [5].

V. Conclusion

In this paper, the harmonics induced by the dead time in the single-phase full-bridge transformerless PV inverter with two modulation schemes (i.e., bipolar and unipolar PWM strategies) were explored. It has been revealed that the harmonic distributions will be affected by the employed modulation strategy. Simulations and experiments validated the discussion, where a harmonic compensator using a repetitive controller was exemplified on a single-phase full-bridge inverter system. The performance of the harmonic compensation scheme is independent of the modulation scheme, since it does not require the information about dominant harmonic induced by the dead time. As a future study, more theoretical analysis will be performed.

Acknowledgment

This work was supported in part by the European Commission within the European Union's Seventh Framework Program (FP7/2007-2013) through the SOLAR-ERA.NET Transnational Project (PV2GRID), by Energinet.dk (ForskEL, Denmark, Project No. 2015-1-12359), and in part by the Research Promotion Foundation (RPF, Cyprus, Project No. KOINA/SOLARERA.NET/0114/02). The study was also supported by the European Research Council (ERC) under the European Unions Seventh Framework Program (FP/20072013)/ERC Grant Agreement [321149-Harmony]. The authors would like to thank the above organizations for the support.

References

[1] F. Blaabjerg, Y. Yang, D. Yang, and X. Wang, "Distributed power-generation systems and protection," *Proceedings of the IEEE*, vol. 105, no. 7, pp. 1311–1331, Jul. 2017.

[2] J. H. R. Enslin and P. J. M. Heskes, "Harmonic interaction between a large number of distributed power inverters and the distribution network," *IEEE Trans. Power Electron.*, vol. 19, no. 6, pp. 1586–1593, Nov. 2004.

[3] S. Muller, J. Meyer, and P. Schegner, "Characterization of small photovoltaic inverters for harmonic modeling," in *Proc. of ICHQP*, pp. 659-663, May 2014.

[4] Y. Yang, K. Zhou, and F. Blaabjerg, "Current harmonics from single-phase grid-connected inverters – examination and suppression," *IEEE J. Emerg. Sel. Top. Power Electron.*, vol. 4, no. 1, pp. 221–233, Mar. 2016.

[5] K. Zhou, D. Wang, Y. Yang, and F. Blaabjerg, *Periodic Control of Power Electronic Converters*, ser. Energy Engineering. Institution of Engineering and Technology, 2016.

[6] X. Yuan, W. Merk, H. Stemmler, and J. Allmeling, "Stationary-frame generalized integrators for current control of active power filters with zero steady-state error for current harmonics of concern under unbalanced and distorted operating conditions," *IEEE Trans. Ind. Appl.*, vol. 38, no. 2, pp. 523–532, Mar. 2002.

[7] *IEEE Standard for interconnecting distributed resources with electric power systems*, IEEE Std 1547.2-2008, 2009.

[8] J. Meyer, M. Domagk, L. Kirchner, K. Malekian, F. Safargholi, M. Hoven, I. Athamna, M. Muehlberg, F. Scheben, F. Ackermann, R. Klosse, and K. Kuech, "Survey on international practice of calculating harmonic current emission limits," in *Proc. of ICHQP*, pp. 539–544, Oct. 2016.

[9] Z. Zhang and L. Xu, "Dead-time compensation of inverters considering snubber and parasitic capacitance," *IEEE Trans. Power Electron.*, vol. 29, no. 6, pp. 3179–3187, Jun. 2014.

[10] L. Chen and F.-Z. Peng, "Dead-time elimination for voltage source inverters," *IEEE Trans. Power Electron.*, vol. 23, no. 2, pp. 574–580, Mar. 2008.

[11] T. Mannen and H. Fujita, "Dead time compensation method based on current ripple estimation," *IEEE Trans. Power Electron.*, vol. 30, no. 7, pp. 4016–4024, Jul. 2015.

[12] D.-H. Lee and J.-W. Ahn, "A simple and direct dead-time effect compensation scheme in PWM-VSI," *IEEE Trans. Ind. Appl.*, vol. 50, no. 5, pp. 3017–3025, Sept. 2014.

[13] R. Grezaud, F. Ayel, N. Rouger, and J. C. Crebier, "A gate driver with integrated deadtime controller," *IEEE Trans. Power Electron.*, vol. 31, no. 12, pp. 8409–8421, Dec. 2016.

[14] K. Okuda, T. Isobe, H. Tadano, and N. Iwamuro, "A dead-time minimized inverter by using complementary topology and its experimental evaluation of harmonics reduction," in *Proc. of EPE'16 - ECCE Europe*, pp. 1–10, Sept. 2016.

[15] X. Chen, X. Ruan, D. Yang, W. Zhao, and L. Jia, "Injected grid current quality improvement for a voltage-controlled grid-connected inverter," *IEEE Trans. Power Electron.*, vol. 33, no. 2, pp. 1247–1258, Feb. 2018.

[16] S.-H. Hwang and J.-M. Kim, "Dead time compensation method for voltage-fed PWM inverter," *IEEE Trans. Energy Convers.*, vol. 25, no. 1, pp. 1–10, Mar. 2010.

[17] Y. Yang, K. Zhou, H. Wang, and F. Blaabjerg, "Harmonics mitigation of dead time effects in PWM converters using a repetitive controller," in *Proc. of APEC*, pp. 1479–1486, Mar. 2015.

[18] N. Mohan, T.M. Undeland, and W.P. Robbins, *Power Electronics: Converters, Applications, and Design*, 3rd ed. John Wiley & Sons, Inc., 2003.

[19] S. Ahmed, Z. Shen, P. Mattavelli, D. Boroyevich, and K. J. Karimi, "Small-signal model of voltage source inverter (VSI) and voltage source converter (VSC) considering the deadtime effect and space vector modulation types," *IEEE Trans. Power Electron.*, vol. 32, no. 6, pp. 4145–4156, Jun. 2017.

[20] H. S. Kim, Y. C. Kwon, S. J. Chee, and S. K. Sul, "Analysis and compensation of inverter nonlinearity for three-level T-type inverters," *IEEE Trans. Power Electron.*, vol. 32, no. 6, pp. 4970–4980, Jun. 2017.

[21] A.R. Munoz and T.A. Lipo, "On-line dead-time compensation technique for open-loop PWM-VSI drives," *IEEE Trans. Power Electron.*, vol. 14, no. 4, pp. 683–689, Jul. 1999.

[22] M.A. Herran, J.R. Fischer, S.A. Gonzalez, M.G. Judewicz, and D.O. Carrica, "Adaptive dead-time compensation for grid-connected PWM inverters of single-stage PV systems," *IEEE Trans. Power Electron.*, vol. 28, no. 6, pp. 2816–2825, Jun. 2013.

[23] Z. Tang and B. Akin, "Suppression of dead-time distortion through revised repetitive controller in PMSM drives," *IEEE Trans. Energy Convers.*, vol. 32, no. 3, pp. 918–930, Sept. 2017.

[24] R. Teodorescu, M. Liserre, and P. Rodríguez, *Grid Converters for Photovoltaic and Wind Power Systems*, ser. Wiley - IEEE. Wiley, 2011.